Journal of Alloys and Compounds 503 (2010) L40–L43

Contents lists available at ScienceDirect

Journal of Alloys and Compounds

journal homepage: www.elsevier.com/locate/jallcom

Letter

Fabrication of well-aligned and dumbbell-shaped hexagonal ZnO nanorod arrays and their dye sensitized solar cell applications

Ahsanulhaq Qurashi[a,b,*], M.F. Hossain[b], M. Faiz[c], N. Tabet[c], Mir Wakas Alam[d], N. Koteeswara Reddy[e]

[a] Center of Research Excellence in Nanotechnology and Department of Chemistry at King Fahd University of Petroleum and Minerals, Dhahran, Saudi Arabia
[b] School of Engineering, University of Toyama, 3190 Gofuku, Toyama 930-8555, Japan
[c] Surface Science Laboratory, Physics Department, and Center of Research Excellence in Nanotechnology at King Fahd University of Petroleum and Minerals, Dhahran, Saudi Arabia
[d] Department of Physics, Fergusson College, Pune 411004, Maharashtra, India
[e] Department of Nanobio Materials and Electronics, GIST, Gwangju 500712, South Korea

ARTICLE INFO

Article history:
Received 21 January 2010
Received in revised form 4 May 2010
Accepted 5 May 2010
Available online 11 May 2010

Keywords:
ZnO
Dumbbell-shaped nanorods
Aligned nanorods
Solution method
Dye sensitized solar cell

ABSTRACT

Dumbbell-shaped hexagonal and well-aligned ZnO nanorod arrays (NRAs) were fabricated by simple and low temperature aqueous solution technique on ZnO-coated FTO substrate and in solution respectively. Structural analysis revealed an excellent crystal quality and wurtzite hexagonal structure of ZnO nanostructures. ZnO nanostructures were used as the wide band gap semiconducting photoelectrode in dye-sensitized solar cells (DSSCs). Well-aligned ZnO NRAs were greatly enhances dye adsorption, leading to improved light harvesting and overall efficiencies. Solar cells made from aligned ZnO NRAs showed photocurrents of 2.08 mA/cm^2, internal quantum efficiencies of 34.5%, and overall efficiencies of 0.32%. However, DSSC made from the randomly formed dumbbell-shaped hexagonal ZnO nanorods showed efficiency about 0.26%, with internal quantum efficiency of 31.5% respectively.

1. Introduction

One-dimensional (1D) metal-oxide nanostructures attracted considerable attention due to their potential applications in present and future nanodevices. Among them, zinc oxide (ZnO) with a wurtzite crystal structure investigated broadly. ZnO 1D nanostructures have received extensive interest in room-temperature ultraviolet (UV) lasers, chemical sensors, electronic devices, photodetectors and dye-sensitized solar cells (DSSCs), etc. [1–11]. The properties of ZnO nanostructures robustly depend on their dimensions and morphologies. Various morphologies of ZnO nanostructures such as belts, wires, rods, and tubes have been synthesized by different approaches [12–17]. Consequently, an exploration of ZnO nanostructures in aligned arrays is of substantial value for the advancement of novel nanodevices.

For the fabrication of well-aligned ZnO nanostructures, high temperatures methods are mainly used [18–20]. Even though these methods can generate high-quality aligned ZnO nanostructures, they require high temperature and metal catalyst particles to initiate the aligned growth. As a result, such precincts enthused the research on wet chemical synthesis which offers a great potential for a low-cost and large-scale fabrication. The low-temperature wet chemical synthesis methods are predominantly attractive due to their low energy necessities, and environmentally pleasant in nature. Presently large-scale of the research is focused on low temperature methods of ZnO nanostructures due to their easy scale-up. Earlier we reported the growth of well-aligned ZnO nanostructures on patterned and unpatterned silicon substrates [4,15].

1D ZnO nanostructures, a wide-band-gap (3.37 eV) and a large exciton binding energy of 60 meV at room temperature, is a proficient substitute semiconductor to the TiO_2. There are few fascinating reasons which focus the attention of researchers on ZnO including the close band gap and the energetic position of the valence band maximum and conduction band minimum to that of TiO_2. Wurtzite hexagonal structure of ZnO helps for the generation of well-aligned ZnO nanostructures. ZnO also presents superior electron transport contrast with TiO_2 [21]. ZnO nanorod arrays (NRAs) as the photoelectrodes shows a higher conversion efficiency compared to those using the disorderedly nanostructured films [22–26]. In particular, the directionality of transport of the injected electron through the vertical nanorods is expected to be very high. Herein, we demonstrated DSSCs performance of dumbbell-shaped hexagonal nanorods and well-aligned ZnO NRAs. The NRAs were synthesized by a two-step sequential seeding with ZnO thin film and growth in aqueous solution.

* Corresponding author at: School of Engineering, University of Toyama, 3190 Gofuku, Toyama 930-8555, Japan. Fax: +81 76 445 6734.
E-mail address: ahsanulhaq06@gmail.com (A. Qurashi).

0925-8388/$ – see front matter © 2010 Elsevier B.V. All rights reserved.
doi:10.1016/j.jallcom.2010.05.022

Table 1
Photovoltaic performances of and dumbbell-shaped hexagonal and well-aligned ZnO NRAs.

Sample name	V_{OC} (mV)	J_{SC} (mA/cm^2)	FF (%)	η (%)
Dumbbell-shaped hexagonal ZnO nanorods	458	2.32	24.5	0.26
Well-aligned ZnO nanorod arrays	420	2.08	35.6	0.32

2. Experimental details

Two types of ZnO nanostructured samples were prepared by simple procedure. The ZnO seed layer was grown on the FTO substrate with a thickness of ~100 nm by using the sputtering system. For preparing ZnO aligned NRAs, the zinc nitrate hexahydrate and water-soluble hexamethylene tetramine (HMTA) were used as reagents. In a typical reaction, 0.01 M aqueous solution of zinc nitrate hexahydrate ($Zn(NO_3)_2{\cdot}6H_2O$) and HMTA ($C_6H_{12}N_4$) were transferred into pyrex glass bottle and kept in laboratory oven. The FTO glass substrate is immersed upside down in the pyrex glass bottle. The pH of the solution, measured with a portable pH meter (Orion 290A), was maintained at 7. The oven was heated to a temperature of 70 °C and fixed during reaction period of 6 h. After the successful process, the system was cooled to the room temperature. The removed substrates from the aqueous solution was rinsed with distilled water and dried overnight at room temperature. In another experiment similar amount of zinc nitrate hexahydrate and HMTA was placed inside the pyrex bottle and the reaction was carried at 70 °C for 6 h. After the reaction, the flask was cooled to the room temperature. Finally, the precipitates of ZnO were separated from the solution by centrifuging for 8 min with a rotation speed of 8000 rpm and then washed using de-ionized water. The rinse process was repeated three times in order to remove organic and inorganic ions adsorbed on the surface of ZnO completely. The final product in white grayish color was dried in an oven at 60 °C for 24 h.

The crystal structures of the ZnO nanostructures were analyzed by X-ray diffractometer (XRD) with Cu Kα radiations. The morphology of as-grown ZnO nanostructures arrays was examined using field emission scanning electron microscopy (FESEM). Both types of ZnO nanostructured samples were sensitized in dye [cis-di(thiocyanate)bis(2,20-bipyridyl-4,40-di-carboxylate) ruthenium (II)] for 24 h at room temperature. The DSSCs were fabricated by clamping the dye-sensitized ZnO nanostructured film against carbon counter electrode and filling with the capillary force by the electrolyte of 0.5 M KI/0.05 M I2/0.05 M 4-tert butylpridine [27]. The active cell area was 0.25 cm^2. The intensity of light was 100 mW/cm^2. The photovoltaic performances of DSSCs were measured using a Keithley Model-2400 source measure unit and monochromator (SG-80, Yokogawa).

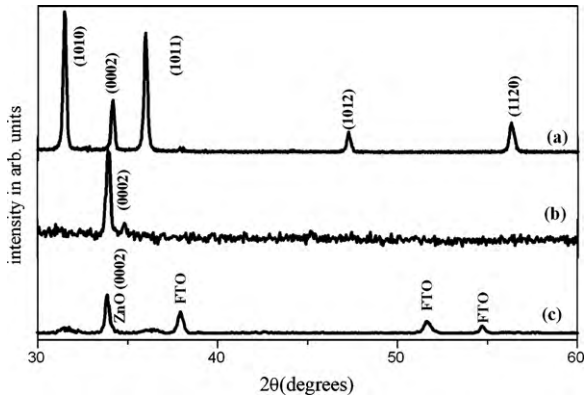

Fig. 1. XRD spectrum of (a) dumbbell-shaped hexagonal, (b) well-aligned ZnO NRAs and (c) XRD spectrum of ZnO-coated FTO glass substrate.

3. Results and discussion

3.1. Crystal structure and surface morphology of ZnO nanostructures

Fig. 1(a) and (b) shows the X-ray diffraction patterns for ZnO nanostructures grown on ZnO-coated FTO substrate and solution respectively. All the diffraction peaks can be indexed to the hexagonal wurtzite phase of ZnO. Fig. 1(a) demonstrates XRD pattern for dumbbell-shaped hexagonal ZnO nanorods which showed various intense peaks related to good crystal quality. Fig. 1(b) shows XRD pattern of ZnO NRAs where the intense peak is (0 0 0 2), indicating an upstanding ZnO NRAs. The (0 0 0 2) peak is related to the crystal plane of wurtzite ZnO while [0 0 0 1] is the growth direction. Fig. 1(c) shows XRD spectrum of ZnO seed layer grown on FTO glass substrate. It is found that the after the growth of NRAs on seeded FTO substrate the peak intensity of (0 0 0 2) increased noticeably.

Fig. 2(a) shows low-magnification FESEM image of ZnO nanostructures grown in the solution without any substrate. The hexagonal nanorods with smooth surfaces can be very well seen in Fig. 2(b). The centre of each nanorod has a narrow neck-like structure which gives it dumbbell-like shape. Each nanorod has

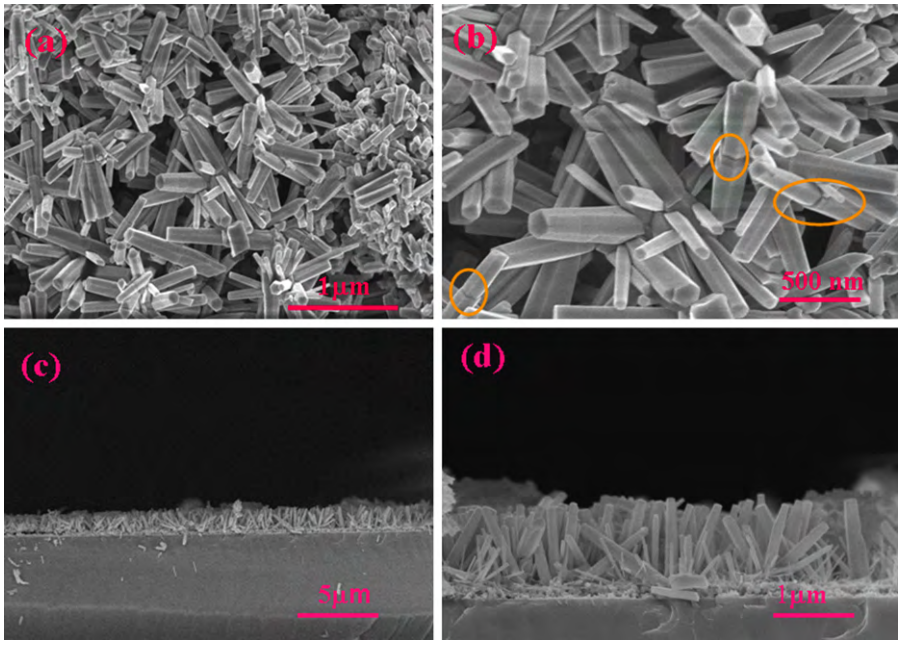

Fig. 2. (a) and (b) Low- and high-magnification FESEM images of dumbbell-shaped hexagonal, (c) and (d) well-aligned ZnO NRAs.

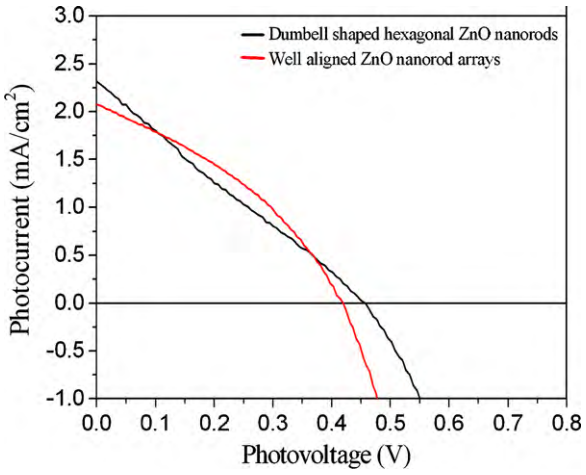

Fig. 3. Photovoltage–photocurrent characteristics of dumbbell-shaped hexagonal and aligned ZnO NRAs based DSSCs.

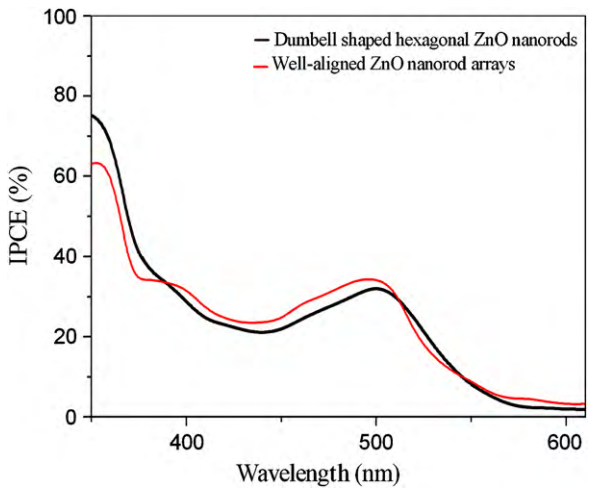

Fig. 4. IPCE spectrum of dumbbell-shaped hexagonal and aligned ZnO NRAs based DSSCs.

a dumbbell-shape indicated by circle in Fig. 2(b). The diameter and length of these nanorods are in between 150–200 nm and 700 nm to 1 μm respectively. Fig. 2(c) and (d) shows low- and high-magnification FESEM images of well-aligned ZnO NRAs grown on ZnO-coated FTO substrate. The FESEM images reveal that the nanorods formed are perpendicular to the surface and grown in a very high-density over the entire surface of ZnO coated FTO substrate. It is fascinating to note that all the grown nanorods possess a perfect hexagonal surface throughout their lengths, which indicates partially that the nanorods are hexagonal in crystal structure, and preferentially grown along the *c*-axis direction. The typical average diameter and length of the as-grown nanorods are 100–200 nm and 1–2 μm, respectively. The ZnO nanorods grown in solution showed hexagonal dumbbell-like morphology as compared to the aligned NRAs grown on ZnO-coated FTO substrate. The aligned growth on ZnO-coated FTO substrate can be attributed to the *c*-axis oriented nature of ZnO seed layer. The seed layer helps the growth of NRAs perpendicular along the substrate as described elsewhere [12–17]. Conversely in solution, anisotropic growth of ZnO nanorods occurs randomly into the different directions due to the absence of any template or seeded substrate. However, recently we found that lithographic patterning can also help to tailor the growth into quasi-aligned direction on cover glass substrate [28].

3.2. Dye sensitized solar cell applications of ZnO nanostructures

The current density–voltage (*J*–*V*) characteristics for a dye-sensitized solar cell fabricated with the dumbbell-shaped hexagonal and ZnO NRAs are shown in Fig. 3. The solar cell conversion efficiency (η) is given as $\eta = (J_{SC} \times V_{OC}/P_{in})$. Here J_{SC} is the short-circuit current density, V_{OC} is the open-circuit voltage, FF is the fill-factor, and P_{in} is the incident light power. In case of dumbbell-shaped hexagonal ZnO nanorods the J_{SC}, V_{OC}, FF, and η (shown in Table 1) were 2.32 mA/cm^2, 458 mV, 24.5 and 0.26% respectively. For the ZnO NRAs DSSCs, the J_{SC}, V_{OC}, FF, and η (shown in Table 1) were 2.08 mA/cm^2, 420 mV, 35.6 and 0.32% respectively. A significant improvement in efficiency is achieved by changing the semiconductor nanostructures morphology from branched dumbbell-shaped nanorods into oriented arrays. This improvement in the overall efficiency can be attributed to the adsorption of dye. The dumbbell-shaped nanorods have thicker layer and due to lack of gaps between the nanorods the dye adsorption seems to be minimal. Conversely the thickness of well-aligned ZnO NRAs was smaller, however, they have small gaps between them as can be seen in Fig. 2(d). These gaps might have ensured the maximum absorption of dye molecules which enhances overall efficiency of NRAs device. Also the geometry of NRAs on substrate plays crucial role for the device performance [2].

The incidence photon to current conversion efficiency (IPCE) as a function of the wavelength of monochromatic irradiation is shown in Fig. 4 [29]. The maximum IPCE of DSSCs was 31.2% for dumbbell-shaped hexagonal and 34.5% for aligned ZnO NRAs. The IPCE spectrum showed two peaks at 405 and 535 nm, which are close to ruthenium based dye (N3-dye) absorption maximum as indicated in Fig. 4.

4. Conclusion

In summary dumbbell-shaped hexagonal and well-aligned ZnO NRAs were prepared by simple aqueous solution chemical synthesis. The FESEM analysis showed excellent growth of aligned and dumbbell-shaped ZnO nanorods. XRD spectrum showed that ZnO nanostructures were wurtzite hexagonal crystal structure with good crystal quality. The two different ZnO nanostructured films were used to assemble the DSSCs. Solar cells made from well-aligned ZnO NRAs showed photocurrents of 2.08 mA/cm^2, fill-factor 34 internal quantum efficiencies of 34.5%, and overall efficiencies of 0.32%. Solar cells made from randomly oriented dumbbell-shaped hexagonal ZnO nanorods show 0.26%, with internal quantum efficiency of 31.5% respectively.

References

[1] M.H. Huang, S. Mao, H. Feick, H. Yan, Y. Wu, H. Kind, E. Weber, R. Russo, P. Yang, Science 292 (2001) 1897–1899.
[2] Q. Ahsanulhaq, J.H. Kim, Y.B. Hahn, Nanotechnology 18 (2007) 485307.
[3] N.K. Reddy, Q. Ahsanulhaq, Y.B. Hahn, App. Phys. Lett. 93 (2008) 083124–083126.
[4] Q. Ahsanulhaq, S.H. Kim, Y.B. Hahn, J. Alloys Compd. 484 (2009) 17–20.
[5] Q. Wan, Q.H. Li, Y.J. Chen, T.H. Wang, X.L. He, J.P. Li, C.L. Lin, Appl. Phys. Lett. 84 (2004) 3654–3656.
[6] A. Qurashi, N. Tabet, M. Faiz, Toshinari Yamazaki, Nanoscale Res. Lett. 4 (2009) 948–954.
[7] J.B. Baxter, E.S. Aydil, Appl. Phys. Lett. 86 (2005) 053114–053116.
[8] J.B. Baxter, A.M. Walker, K.V. Ommering, E.S. Aydil, Nanotechnology 17 (2006) S304.
[9] P. Ravirajan, M.A. Peiro, K.M. Nazeeruddin, M. Graetzel, C.C.D. Bradley, R.J. Durrant, J. Nelson, J. Phys. Chem. B 110 (2006) 7635–7639.
[10] M. Law, L.E. Greene, A. Radenovic, T. Kuykendall, J. Liphardt, P. Yang, J. Phys. Chem. B 110 (2006) 22652–22663.
[11] Q. Ahsanulhaq, J.H. Kim, J.S. Lee, Y.B. Hahn, Electrochem. Commun. 12 (2010) 475–478.
[12] Q. Ahsanulhaq, S.H. Kim, Y.B. Hahn, J. Phys. Chem. Sol. 70 (2009) 627–631.
[13] R.M. Wang, Y.J. Xing, J. Xu, D.P. Yu, New J. Phys. 5 (2003) 115.1–115.7.

[14] Y. Wei, Y. Ding, C. Li, S. Xu, J.H. Ryo, R. Dupuis, A.K. Sood, D.L. Polla, Z.L. Wang, Phys. Chem. C 112 (2008) 18935–18937.
[15] Q. Ahsanulhaq, A. Umar, Y.B. Hahn, Nanotechnology 18 (2007) 115603.
[16] L. Greene, M. Law, D.H. Tan, M. Montano, J. Goldberger, G. Somorjai, P. Yang, Nano Lett. 5 (2005) 1231–1236.
[17] L. Greene, M. Law, J. Goldberger, F. Kim, J.C. Johnson, Y. Zhang, R.J. Saykally, P. Yang, Angew. Chem. Int. Ed. 42 (2003) 3031–3034.
[18] Y.J. Park, J.D. Lee, S.S. Kim, Nanotechnology 16 (2005) 2044.
[19] X. Wang, C.J. Summers, Z.L. Wang, Nano Lett. 4 (2004) 423–426.
[20] J.J. Wu, S.C. Liu, Adv. Mater. 14 (2002) 215–218.
[21] D.I. Suh, S.Y. Lee, T.H. Kim, J.M. Chun, E.K. Suh, O.B. Yang, S.K. Lee, Chem. Phys. Lett. 442 (2007) 348–353.
[22] M. Law, L.E. Greene, J.C. Johnson, R. Saykally, P.D. Yang, Nat. Mater. 4 (2005) 455–459.
[23] Y. Gao, M. Nagai, Langmuir 22 (2006) 3936–3940.
[24] C.Y. Jiang, X.W. Sun, G.Q. Lo, D.L. Kwong, J.X. Wang, Appl. Phys. Lett. 90 (2007) 263501–263503.
[25] W. Yang, F. Wan, S. Chen, C. Jiang, Nanoscale Res. Lett. 4 (2009) 1486–1492.
[26] E. Galoppini, J. Rochford, H. Chen, G. Saraf, Y. Lu, A. Hagfeldt, G. Boschloo, Phys. Chem. B 110 (2006) 16159–16161.
[27] L. Xu, Q. Chen, D. Xu, J. Phys. Chem. C 111 (2007) 11560–11565.
[28] Q. Ahsanulhaq, J.H. Kim, J.H. Kim, Y.B. Hahn, Nanoscale Res. Lett. 5 (2010) 669–674.
[29] M.F. Hossain, S. Biswas, T. Takahashi, Thin Solid Films 517 (2008) 1294–1300.